AERODYNAMICS OF TURBINES

by

Dr. William E. Thompson
Vice President
Turbo Research, Inc.
West Chester, Pennsylvania

William E. Thompson is the Vice President of Turbo Research Inc. He is responsible for all activities in the area of fluid mechanics including turbomachinery aerodynamic performance. He has also worked for Drexel Institute of Technology as an associate professor of mechanical engineering, and at Cornell Aeronautical Laboratories as a principal mechanical engineer.

He received a B.S. degree in mechanical engineering from Carnegie Institute of Technology in 1967, a M.S. degree in mechanical engineering from University of Michigan in 1949, and a Ph.D. degree in mechanical engineering from Illinois Institute of Technology in 1958.

He is a member of several professional societies. He is also a registered professional engineer in the state of New York, and has several publications in the area of compressors and turbines.

ABSTRACT

The transformation between work and other forms of energy is accomplished in turbomachinery. The ability of a turbine to produce work when handling a compressible fluid and when taking either its axial or radial configuration is presented for the user of the equipment rather than the designer or research worker.

The basic conservation principles of mass, linear momentum, energy, and angular momentum in their steady, one-dimensional form are summarized; the figures of merit of turbine stage performance including efficiency, reaction and reheat are defined and interrelated. Correlation of losses with performance parameters is presented first for the over-all stage. Then the Soderberg correlation is provided for handling the axial stage, component by component, and the Benson correlation is introduced for use with a radial stage. An example lists all of the parameters and flow conditions which can be predicted for a prospective design or evaluated for an existing unit of hardware.

INTRODUCTION

Turbomachinery is commonly used to bring about the transformation between work and other forms of energy including internal, potential, and kinetic energy, and to a much lesser extent, heat. As a transformer of energy, turbomachinery plays an important part in industrial processes and systems. It is to the designer and operator of such systems, who must be able to set realistic specifications and verify achievable performance, that this paper is directed.

The apparatus in which the transformation from work to the other energy forms takes place is called a pump when handling incompressible fluids and a compressor when handling compressible fluids. Conversely, the transformation of the various energy forms into work occurs in a turbine regardless of the compressibility or incompressibility of the working fluid. We shall be concerned only with turbines handling compressible fluids in this paper.

The production of work by a turbine depends upon its ability to first produce then reduce the angular momentum of the working fluid. Where a large mass flow is handled by the turbine, the angular momentum change can be carried out at essentially a constant radial position from the rotor axis of rotation: such a configuration is an axial turbine. However, where only a small mass flow is available to the turbine, a reduction in both tangential velocity component and radial position of the fluid is necessary to realize the greatest possible angular momentum change; the resulting configuration is an inward radial flow turbine. After considering the concepts which are applicable in general to both turbine types, we shall develop the loss correlations in parallel for the axial and radial turbine.

Since every effort has been made to make the paper self-contained, the subject has been circumscribed. An account of the performance, design methods and procedures, research efforts and unsolved problems would comprise a monograph or book on each turbine type. As a consistent continuation of the work on axial turbines, the book by Horlock[1] is recommended to the reader. No comparable book exists on the radial turbine but the monograph by Mizumachi[2] is suggested.

DESCRIBING EQUATIONS

We begin with the describing equations. The principles of the conservation of mass, linear and angular momentum, and energy describe the fluid flow phenomena in turbomachine components. The formulations of these principles are often misleadingly called the governing equations even though, of course, they exert no influence on the fluid dynamic events.

A general view with nomenclature of an element of a turbomachine passage is shown in Figure 1. A complete list of the nomenclature used in the paper appears in section I. In Figure 1, the passage is oriented with respect to a cylindrical coordinate system (r, ϑ, z). The unit vector in the r-direction is i, rotating i 90° in the positive ϑ-direction locates j. Perpendicular to the plane formed by i and j is the unit vector k in the z-direction, shown positive in the figure. Rotation of the turbomachine rotor takes place about the z-axis and is considered positive in the sense of positive ϑ. A fluid particle p

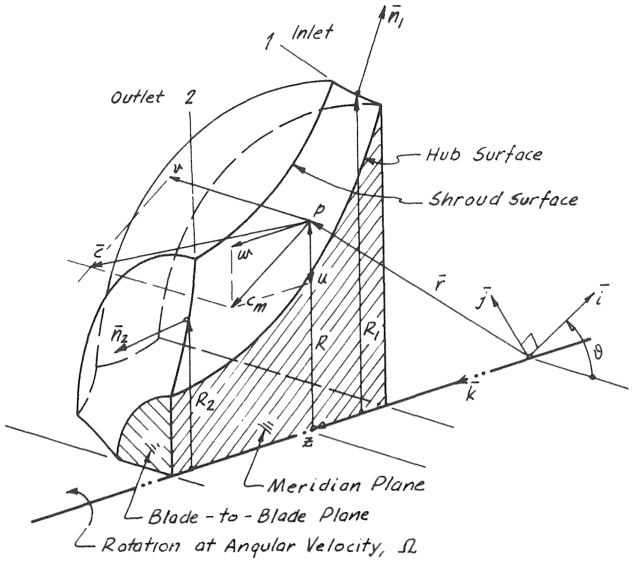

Figure 1. Flow Along a Surface of Revolution in a Turbomachine.

located at a radius R by the radius vector r from the origin moves with the velocity c. The components of the velocity in the three coordinate directions are u, v, w, respectively. However, these velocity components are usually replaced by a more convenient group in the turbomachinery context. The tangential or blade-to-blade component of c is denoted c_u and the meridional component of c, which is the resultant of u and w, is denoted c_m. Then u is used to denote the rotor tangential velocity at the point in question ($u = c_u$) and w indicates the particle velocity relative to a coordinate system rotating with the angular velocity of the rotor. Finally, n is a unit vector positive in the sense of being outward drawn from the surface to which it is perpendicular. Thus, at the inlet station (1), n_1 is parallel to c_1 but of opposite sense while at (2), n_2 and c_2 are parallel and of the same sense.

The formulation of the conservation of mass principle is summarized in Table 1a. We do not look at discrete particles but rather at a continuum of particles

$$M \equiv \int_{system} \rho \, dv$$

$$(DM/Dt)_{system} = 0$$

$$\partial/\partial t \int_V \rho \, dv + \int_S (\bar{n} \cdot \rho \bar{c}) \, da = 0$$

$$\partial \rho/\partial t + \nabla \cdot \rho \bar{c} = 0$$

for one-dimensional, steady flow:

$$\boxed{\rho c A = \text{constant} \equiv \dot{m}}$$

Table 1a. Conservation of Mass Principle (Continuity Equation).

comprising the system moving through the turbomachine passage. The mass of the system is defined by eq. (1). The conservation of mass of that system is expressed by eq. (2). The conditions of the system moving through the passage are then related to conditions in the flow as observed from a fixed position by means of Reynolds Transport Theorem. Application of this theorem results in eq. (3) which is a useful, integral formulation of the principle. The principle in the form of a differential equation appears in eq. (4) where an appropriate form of Green's Theorem relating area and volume integrals was used to first modify eq. (3). The simplification to steady, one-dimensional flow is most important to our present interests. For steady flow, changes with respect to time do not occur ($\partial/\partial t = 0$); for one-dimensional flow, changes in flow conditions occur only in the direction of flow. The second integral in eq. (3) can then be evaluated with the result shown in eq. (5). The useful forms, eq. (3), (4) and (5) are each often called the continuity equation.

The reader must realize that the equations in Table 1a do not constitute a derivation of eq. (5) but they are a reminder of the important ideas behind the existence of eq. (5). A more complete explanation and derivation can be found in the basic reference books by Shapiro[3], Daily and Harleman[4], Owczarek[5], and Thompson[6]. The comments apply equally to the other parts of Table 1.

A summary of the principle of conservation of linear momentum appears in Table 1b. After defining the momentum of the system in eq. (6), we see that it can be changed by the application of body and surface forces. The principle is expressed in eq. (7) and is just Newton's second law of motion. The integral form for fixed coordinates is given in eq. (8) where an important simplification has been introduced. Surface forces arise from the application of stress to the surface. Such stress is, in general, both normal (pressure) and tangential (shear) to the surface. Here the shear stress is omitted

$$\bar{P} \equiv \int_{system} \rho \bar{c} \, dv \qquad (6)$$

$$(D\bar{P}/Dt)_{system} = (\bar{F}_{surface} + \bar{F}_{body})_{system} \qquad (7)$$

$$\partial/\partial t \int_V \rho \bar{c} \, dv + \int_S \bar{c} (\bar{n} \cdot \rho \bar{c}) \, da = -\int_S p \bar{n} \, da + \int_V \rho \bar{g} \, dv \qquad (8)$$

$$\partial \bar{c}/\partial t + (\bar{c} \cdot \nabla)\bar{c} = -\nabla p/\rho + \bar{g} \quad \text{(Euler's Equation)} \qquad (9)$$

for one-dimensional, steady rotational flow along streamline, or irrotational flow throughout field:

$$\boxed{c^2/2 + \int \frac{dp}{\rho} + \bar{\psi} = \text{constant}} \quad \text{(Bernoulli Equation)} \qquad (10)$$

Since $dp/\rho \equiv dh - T ds$, when $ds = 0$,

$$\boxed{c^2/2 + h + \bar{\psi} = h_o} \qquad (11)$$

Table 1b. Conservation of Linear Momentum Principle (Equations of Motion).

as a consequence of assuming negligible viscosity of the working fluid, and only a surface force due to the pressure appears in eq. (8). Nonetheless, viscosity is at the basis of the existence of losses in turbomachine passages. We shall reintroduce this effect at a later point in this paper by using loss coefficients which modify the results of inviscid flow calculations. The differential form of the equations of motion is given by eq. (9) and is often called Euler's equation. Once again applying the conditions of steady, one-dimensional flow, integration of eq. (8) results in Bernoulli's equation, eq. (10). It is valid for both rotational flow along a streamline and irrotational flow throughout the flow field. If one assumes isentropic flow ($ds = 0$), the integral in eq. (10) becomes the enthalpy and the Bernoulli constant is synonymous with the stagnation enthalpy.

The conservation of energy principle is outlined in Table 1c, where the energy of the system is defined by eq. (12). The principle is well known as the first law of thermodynamics where the change of energy of the system is the net effect of the heat and work transfers, eq. (13). Referred to a fixed observer, we have eq. (14a) and after a considerable calculation, this becomes eq. (14b). It is then convenient to group all the volume integrals and write the differential form eq. (15). Now assuming no heat or work transfer together with steady, one-dimensional flow, we obtain the simplified differential form eq. (16) which is interpreted to be the product of the magnitude of the velocity and the directional derivative of the Bernoulli constant in the direction of the flow. Since the velocity is not zero, the change of the Bernoulli constant along a streamline must be zero. Integrating eq. (16), we can only conclude that the stagnation enthalpy is constant along a streamline, eq. (17).

$$E \equiv \int_{system} \rho e \, d\forall = \int_{system} \rho \left(c^2/2 + e \right) d\forall \tag{12}$$

$$(DE/Dt)_{system} = (\delta Q/\delta t)_{system} + (\delta W/\delta t)_{system} \tag{13}$$

$$D/Dt \int_V \rho e \, d\forall = \dot{Q} - \int_S p(\bar{n} \circ \bar{c}) da + \int_V \rho(\bar{g} \circ \bar{c}) d\forall + \dot{W}_{mech} \tag{14a}$$

$$\int_V \left(\rho \frac{De}{Dt}\right) d\forall + \int_V \left(\frac{D}{Dt}\left(\frac{p}{\rho}\right) - \frac{1}{\rho}\frac{\partial p}{\partial t}\right)\rho \, d\forall + \int_V \left(\frac{D\psi}{Dt} - \frac{\partial \psi}{\partial t}\right)\rho \, d\forall = \dot{Q} + \dot{W}_{mech} \tag{14b}$$

$$\frac{D}{Dt}\left(e + c^2/2 + p/\rho + \psi\right) - \frac{1}{\rho}\frac{\partial p}{\partial t} - \frac{\partial \psi}{\partial t} = \dot{q} + \dot{w}_{mech} \tag{15}$$

for one-dimensional, steady flow with no heat or work transfer

$$\bar{c} \circ \nabla\left(h + c^2/2 + \psi\right) = \bar{c} \circ \nabla h_o = c \frac{dh_o}{ds} = 0 \tag{16}$$

$$\boxed{h_o = h + c^2/2 + \psi = \text{constant}} \tag{17}$$

valid along a streamline; h_o is stagnation enthalpy

Table 1c. Conservation of Energy Principle (First Law of Thermodynamics).

$$\bar{H} \equiv \int_{system} \rho(\bar{r} \times \bar{c}) \, d\forall \tag{18}$$

$$(D\bar{H}/Dt)_{system} = \left(\bar{r} \times \bar{F}_{surface} + \bar{r} \times \bar{F}_{body}\right)_{system} + \bar{M}_{mech} \tag{19}$$

$$\frac{\partial}{\partial t}\int_V \rho(\bar{r} \times \bar{c}) d\forall + \int_S (\bar{r} \times \bar{c})(\bar{n} \circ \rho \bar{c}) da = -\int_S \bar{r} \times p\bar{n} \, da + \int_V \bar{r} \times \rho \bar{g} \, d\forall + \bar{M}_{mech} = \bar{M} \tag{20}$$

Consider the moment about the axis of rotation (z-axis):

$$\bar{T}_z = (\bar{M} \circ \bar{k})\bar{k} = T_z \bar{k} \tag{21}$$

For one-dimensional, steady flow through inlet area A_1 and exit area A_2

$$\bar{T}_z = \left\{ \int_{A_1} \left[(\bar{r} \times \bar{c}) \circ \bar{k}\right](\bar{n} \circ \rho \bar{c}) da + \int_{A_2} \left[(\bar{r} \times \bar{c}) \circ \bar{k}\right](\bar{n} \circ \rho \bar{c}) da \right\} \bar{k}$$

with $(\bar{r} \times \bar{c}) \circ \bar{k} = Rv$ and $\int_A Rv(\bar{n} \circ \rho \bar{c}) da = \rho c A \widehat{Rv} = \dot{m} \widehat{Rv}$

$$\boxed{\bar{T}_z = \dot{m}\left(\widehat{R_2 v_2} - \widehat{R_1 v_1}\right)\bar{k}} \quad \text{Euler's Turbine Formula} \tag{22}$$

$$w_{mech} = \dot{W}_{mech}/\dot{m} = (\Omega \bar{k} \circ T_z \bar{k})/\dot{m} = (\Omega T_z)/\dot{m};$$

for adiabatic flow, the energy equation becomes

$$\boxed{w_{mech} = h_{o1} - h_{o2} = \Omega\left(\widehat{R_1 v_1} - \widehat{R_2 v_2}\right)} \tag{23}$$

for a turbine, $\widehat{R_1 v_1} > \widehat{R_2 v_2}$, hence $h_{o1} > h_{o2}$

for a compressor, $\widehat{R_1 v_1} < \widehat{R_2 v_2}$, hence $h_{o2} > h_{o1}$

Table 1d. Conservation of Angular Momentum Principle (Moment of Momentum).

The form of eqs. (14) and (15) was developed with a view to yielding eq. (17). The reader is advised that many forms of the energy equation are developable for other purposes as is evident in the books referred to above. Our purpose in obtaining eq. (17) was twofold. Under the assumptions identified above, the energy equation and Bernoulli's equation of motion are not independent and unique results, but rather one and the same thing. On the other hand, as pointed out in the introduction, it is the purpose of turbomachinery to effect the transformation between work and other forms of energy. Thus in a rotor passage or in a turbomachine stage which includes a rotor passage, the work term will not be zero, the consequence of which is to change the value of the Bernoulli constant of the flow upon passage through the rotor.

The last of the conservation principles is concerned with angular momentum (moment of momentum) and is summarized in Table 1d. The angular momentum of the system, eq. (18) is just the moment of the linear momentum of the system, eq. (6). In addition to the moments of the body and surface forces, we admit the possibility of mechanical moments or torques, as are encountered in turbomachine applications, having an effect on or being affected by the angular momentum

change of the system, eq. (19). To a fixed observer, the result is eq. (20).

Up to this point we have attempted to present the summaries in the parts of Table 1 with a certain symmetry. It is not possible to carry that idea any further in the present example. The angular momentum principle is usually used for one of two purposes. Had the full stress tensor been included in the linear momentum equation, the conservation of angular mometum could have been used to show that that tensor must be symmetric, a result which has consequences in the study of viscosity and the constitutive equations of the working fluids. Such considerations are outside the scope of the present paper. Of more immediate importance is the use of the angular momentum equation to compute the torque or mechanical work transfer of a turbomachine in which the angular momentum of the flowing fluid is changed.

In eq. (20), the resultant moment of the body force, the surface force and the mechanical torques is a vector quantity with components acting about the three coordinate axes. The components about the axes in the $\bar{i}$ and $\bar{j}$ directions are simply equilibrated by the bearings of a turbomachine rotor. The moment about the z-axis, the axis of rotation of the rotor, is capable of producing a work transfer across the boundaries of the machine. The remainder of Table 1d is devoted to calculating this torque and the mechanical work transfer which results.

The component of the moment about the z-axis is written in general in eq. (21). After applying the simplifications of steady, one-dimensional flow, eq. (22) is easily obtained and is known as Euler's Turbine Formula. The circumflex over the product $\widehat{Rv}$ denotes a "suitable" average. Consistent with the one-dimensional calculations in connection with the previous conservation equations, v (or c_u) is considered constant over the cross-section. Where R is also constant as at the discharge of a radial compressor impeller, no problem arises.

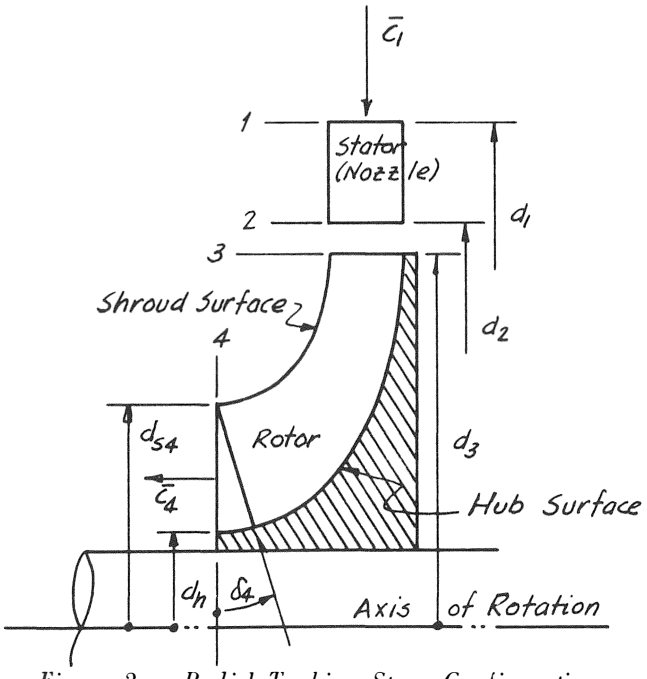

Figure 2a. Radial Turbine Stage Configuration.

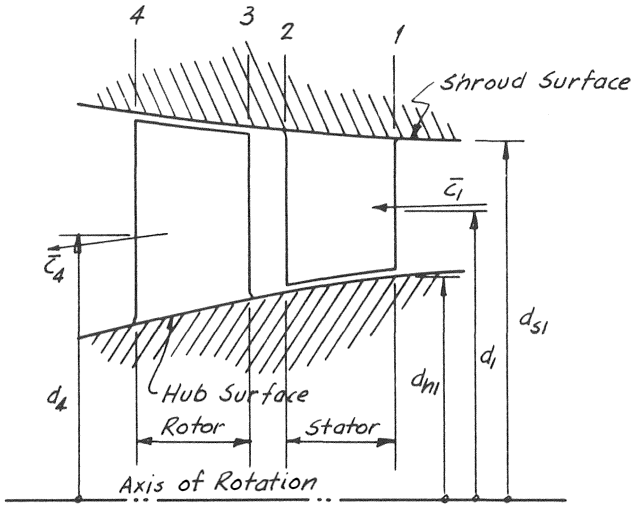

Figure 2b. Axial Turbine Stage Configuration.

Where R varies over the cross-section, as at both the inlet and exit of an axial turbine rotor, a root-mean-square value of R is often used but no generally accepted custom seems to exist. Again if R is the constant tip radius then $\Omega R = u$ and $\Omega R c_u = u c_u$. Remember, however, that only a special average leads to this attractive result.

The mechanical energy or work term for the energy equation may be calculated by dividing the product of the torque and the angular velocity by the mass flow rate. Substituting this result in the energy equation for adiabatic flow (no heat transfer) results in eq. (23), which together with the momentum equation eq. (11) and the continuity equation, eq. (5), is a basic tool of one-dimensional aerodynamic analysis or synthesis.

It should be noted that the work calculated by eq. (23) corresponds to the energy actually yielded by the working fluid but is diminished by three small parasite losses before delivery as shaft work by the turbine. Rotor disk friction returns a small amount of the work as heat to the downstream flow while seal and bearing friction dissipates a small amount of the work which is lost from the system.

FIGURES OF MERIT

Stage Configuration

Before proceeding to summarize the various definitions of efficiency, reaction, etc. and to show their interrelations, we have assembled in Figure 2 sketches of the physical configuration of both a radial and an axial turbine stage, the stage blading and velocity diagrams as well as an enthalpy-entropy diagram on which the stage flow processes can be traced. Corresponding stations (1), (2), (3), and (4) are shown in Figures 2a and 2b for each turbine type. Stations (1) and (2) designate stator or nozzle inlet and exit respectively while stations (3) and (4) specify rotor inlet and exit respectively. Other nomenclature and terms are clearly shown on the figure.

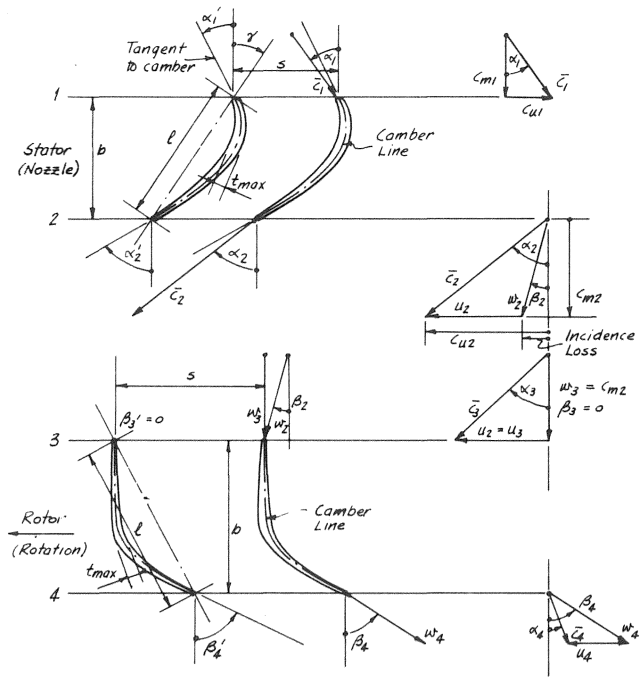

Figure 2c. Stage Nomenclature and Velocity Triangles.

With little effort, Figure 2c can be imagined applicable to both radial and axial turbine types. In each case the gap between stations (2) and (3) is exaggerated to accommodate the velocity diagrams. Two of the many blades in both the stator and the rotor are shown in the figure. To the left, the geometry of the blade profile is illustrated. The stator blade angle α' is measured between a line tangent to the camber line at the blade edge and the direction parallel to the rotor axis (the meridian line). The rotor blade angle measured relative to the moving blade is denoted β and again measured between camber line tangent and meridian line. Other profile dimensions and angles are shown. To the right, the geometry of the gas flow over the blade profile is illustrated. The gas velocity $\bar{c}$ makes an angle α at the stator blade edge and is measured with respect to the meridian line. The gas relative velocity w makes an angle β at the rotor blade edge and is measured with respect to the meridian line. Other components of the gas velocity and the rotor tangential velocity are shown on the velocity diagrams.

The distinction between the blade angle and the gas angle at the same station has been emphasized above because a difference at the blade leading edge, say, of the gas flow direction and the blade camber line results in flow at incidence and a loss occurs. At the blade trailing edge, similar misalignment is called a deviation. To complete the nomenclature the sum of the blade angles is called the blade camber while the sum of the gas angles about a blade describes the turning of the flow and is called the deflection. Expressions for these terms for both stator and rotor are included in Figure 2c.

Stage h-s Diagrams

Perhaps the most important diagram for describing the flow phenomena in a turbine stage at our present level of one-dimensional flow analysis and loss correlation is the enthalpy-entropy diagram for the stage shown in Figure 2d. Station numbers on this diagram coincide with those on the previous parts of Figure 2. Two lines denoting the flow process are shown even though, of course, only one process takes place. The top line connects stagnation conditions at the several stations while the lower line denotes the static conditions. Notice that the same entropy value is applicable to both static and stagnation conditions at a given station. Also note that an actual process terminates in an unprimed station number while the same process under ideal isentropic conditions would have terminated at the station designated by the corresponding single primed number.

Isentropic Efficiency and Reaction

There are numerous parameters by which the ability of a turbine to convert energy into mechanical work can be judged. As a group they may be designated figures of merit and we shall guard against allowing the group to become too large.

A summary of the formulations of the figures of merit is given in Table 2. Eqs. (24), (25) and (26) comprise the definitions of the stator or nozzle efficiency,

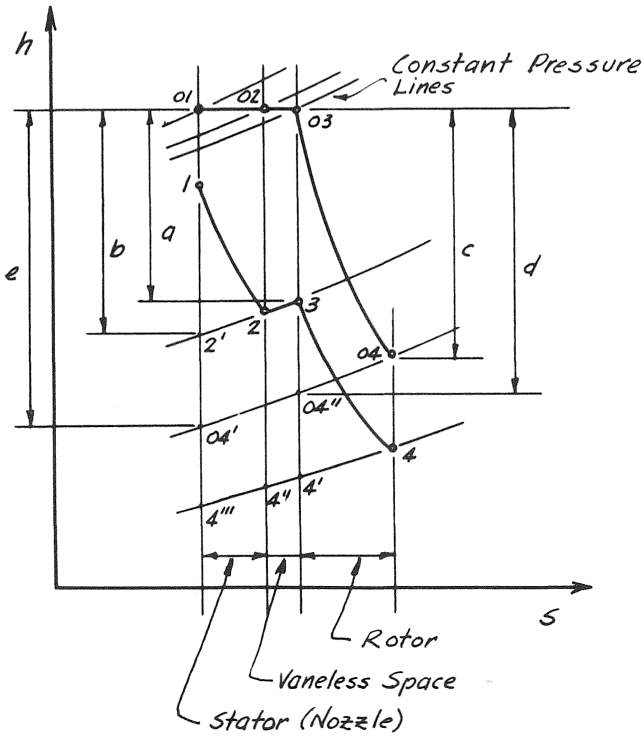

Figure 2d. h-s Diagram for Turbine Stage Process.

Nozzle Efficiency: $$\eta_N \equiv \frac{a}{b} = \frac{h_{03} - h_3}{h_{01} - h_{3'}} \quad (24)$$

Rotor Efficiency: $$\eta_R \equiv \frac{c}{d} = \frac{h_{03} - h_{04}}{h_{03} - h_{04''}} \quad (25)$$

Turbine Stage Isentropic Efficiency: $$\eta_T \equiv \frac{c}{e} = \frac{h_{03} - h_{04}}{h_{01} - h_{04'}} \quad (26)$$

Assume that constant pressure lines are parallel on h-s diagram

$$h_{3'} - h_{04'} \cong h_3 - h_{04''} = (h_{03} - h_{04''}) - (h_{03} - h_3) \quad (27)$$

$$\frac{h_{01} - h_{04'}}{h_{01} - h_{04}} = \frac{h_{01} - h_{3'}}{h_{03} - h_{04}} + \frac{h_{03} - h_{04''}}{h_{03} - h_{04}} - \frac{h_{03} - h_3}{h_{03} - h_{04}}$$

$$\frac{1}{\eta_T} = \frac{1}{\eta_R} + \frac{h_{03} - h_3}{h_{03} - h_{04}} \left(\frac{h_{01} - h_{3'}}{h_{03} - h_3} - 1 \right) \quad (28)$$

$$\frac{h_{03} - h_3}{h_{03} - h_{04}} = \frac{c_3^2/2 + (h_{03} - h_{04}) - (h_{03} - h_{04})}{h_{03} - h_{04}}$$

$$= 1 - \frac{(h_{03} - h_{04}) - c_3^2/2}{h_{03} - h_{04}} \equiv 1 - r \quad (29)$$

$$\boxed{\frac{1}{\eta_T} = \frac{1}{\eta_R} + (1 - r)\left(\frac{1}{\eta_N} - 1\right)} \quad (30)$$

Table 2a. Figures of Merit: Isentropic Efficiency and Reaction.

the rotor efficiency and the stage isentropic efficiency respectively. The station points at which the enthalpy is evaluated are those shown in Figure 2d. The stage isentropic efficiency is often called the stage adiabatic efficiency. The thermodynamic basis for making such a definition of stage efficiency is discussed by Horlock[1] (Chapter 1).

In general, the slope of the constant pressure lines on the diagram is inversely proportional to the absolute temperature for any gas. Such lines curve upward and diverge slightly at increasing entropy. If a process does not encounter either a large pressure change or a large entropy change, then it is an acceptable approximation to assume that the constant pressure lines are straight and parallel. The approximation in eq. (27) is made on this basis and manipulation of the enthalpy differences produces eq. (28) where the stage and rotor efficiencies are identifiable. Expanding one of the terms in eq. (28) yields eq. (29) in which the degree of reaction of the turbine stage is defined. Putting it all together results in eq. (30), a remarkably simple relation between stage, nozzle and rotor efficiency and the reaction of the stage.

Nozzle and rotor efficiencies have been defined to yield the simple relation eq. (30). Their definition is identical or nearly identical to many appearing in the literature. Originally the reaction of a stage was expressed in terms of the pressure when fluid flow conditions were essentially incompressible. Now it is appropriate to use enthalpy with compressible fluids. The reaction expresses the ratio of static enthalpy change in the rotor ($h_3 - h_1$) to that over the stage ($h_1 - h_1$). It really describes the portion of the expansion taking place in the rotor in comparison to the expansion across the stage. The expression for the reaction in eq. (29) is then recognized if the entering velocity $\bar{c}_1$, and the leaving velocity $\bar{c}_1$ are approximately equal to each other and considered small with respect to $\bar{c}_3$.

Polytropic Efficiency and Reheat

In Table 2b, the definition of the figures of merit of a turbine stage are continued. An incremental enthalpy drop dh_0 occurs across a "small" stage and with this the small stage efficiency is defined in eq. (31). If the small stage efficiency is constant for a large number of increments in a turbine stage, integration throughout the stage yields eq. (32) where the constant efficiency applicable across the stage is called the polytropic efficiency. Comparing terms in eq. (32) leads to eq. (33) where n is the polytropic exponent used to relate the pressure and the temperature in the actual expansion process. Eq. (34), relating the polytropic efficiency to the isentropic efficiency using the stage pressure ratio, is found with a little algebraic manipulation.

Whereas the assumption of straight, parallel constant pressure lines on the h-s diagram led to eq. (30), the retention of their slightly diverging characteristic leads to the stage or turbine reheat factor. The ratio of the sum of the incremental isentropic enthalpy drops through the many "small" stages to a single isentropic

Small Stage Efficiency: $$\eta_s \equiv \frac{dh_0 \text{ actual}}{dh_{0\,\text{isen}}} = \frac{c_p\, dT_0}{dp_0/\rho_0} \quad (31)$$

for an ideal gas: $$\frac{dT_0}{T_0} = \eta_s \left(\frac{\gamma - 1}{\gamma}\right) \frac{dp_0}{p_0}$$

Assume η_s is constant for each increment of integration interval.

$$\frac{T_0}{p_0^{\eta_{PT}\left(\frac{\gamma-1}{\gamma}\right)}} = \frac{T_0}{p_0^{\frac{n-1}{n}}} \quad (32)$$

$$\boxed{\eta_{PT} = \left(\frac{\gamma}{\gamma - 1}\right)\left(\frac{n-1}{n}\right)} \quad (33)$$

Since $$\eta_T = \frac{h_{01} - h_{04}}{h_{01} - h_{04'}} = \frac{1 - \left(\frac{p_{04}}{p_{01}}\right)^{\eta_{PT}\left(\frac{\gamma-1}{\gamma}\right)}}{1 - \left(\frac{p_{04}}{p_{01}}\right)^{\frac{\gamma-1}{\gamma}}}$$

$$\boxed{\eta_{PT} = \frac{\ln\left[1 - \eta_T + \eta_T \left(\frac{p_{04}}{p_{01}}\right)^{\frac{\gamma-1}{\gamma}}\right]}{\left(\frac{\gamma-1}{\gamma}\right) \ln\left(\frac{p_{04}}{p_{01}}\right)}} \quad (34)$$

Divide $(h_{01} - h_{04})$ into many "small stage" steps of equal η_s:

$$(h_{01} - h_{04}) = \eta_T (h_{01} - h_{04'})$$

$$= \eta_s (h_{01} - h_{x'}) + \eta_s (h_x - h_{y'}) + \cdots = \eta_{PT} \Sigma \Delta h_{isen}$$

$$\boxed{\frac{\eta_T}{\eta_{PT}} = \frac{\Sigma \Delta h_{isen}}{h_{01} - h_{04'}} \equiv R_H} \quad \text{the Reheat Factor} \quad (35)$$

$$\boxed{\eta_T = \eta_{PT} R_H} \quad (36)$$

Table 2b. Figures of Merit: Polytropic Efficiency and Reheat.

enthalpy drop over the whole stage is defined as the reheat factor, see eq. (35). Relating the isentropic drops to the actual changes by means of the efficiency, the reheat factor may be expressed as the ratio of the isentropic to the polytropic turbine stage efficiency, eqs. (35) and (36). Since the constant pressure lines diverge at greater entropies, the sum of the small stage isentropic enthalpy drops will be somewhat larger than the single over-all isentropic change from the initial conditions over the same pressure interval. Hence, the reheat factor is somewhat greater than unity. Consequently, the turbine isentropic efficiency is somewhat greater than the turbine polytropic efficiency. In any event, since the polytropic efficiency is less than unity, eq. (33) also shows that the polytropic exponent is greater than the ratio of the specific heats of the gas handled by the turbine.

Fluid Mechanics of a Turbine Stage

Many of the ingredients for a one-dimensional fluid mechanical analysis or synthesis of a turbine stage are now at hand. These include the equations of continuity eq. (5), motion eq. (11), energy eq. (17), conversion between angular momentum and work eq. (23), and the various definitions and interrelations between efficiency, reaction and reheat just summarized. Occasionally some additional knowledge of basic compressible fluid dynamics may be needed in carrying out a stage analysis, knowledge which we will not be able to review here. Reference to Horlock's work[1] is suggested for those interested in axial turbines. Radial turbines do not enjoy as mature a development as axial turbines and no single reference book can be identified. However, a fairly complete account may be constructed from references 2, and 7-18.

However, one important point remains and the balance of this paper is given to its consideration. Referring to Figure 2d, it will be necessary to determine conditions at station (2) from (2′), at (3) from (2), and at (4) from (4′) in order to complete an evaluation of turbine stage performance. These three steps establish actual flow conditions in place of the ideal using correlations of the nozzle loss, the incidence loss and the rotor passage loss respectively.

CORRELATION OF TURBINE EFFICIENCY WITH FLOW CONDITIONS AND STAGE CONFIGURATION

Before we consider the correlation of losses in the individual elements of a turbine stage, we recognize a general correlation of stage performance with flow conditions and stage configuration first suggested by Balje.[19] More recently, Balje and Binsley,[20] assuming that nine independent variables would adequately describe the turbine stage performance, used the method of dimensional analysis to obtain the six dimensionless parameters listed in Table 3. Balje[19] found previously that efficiency was primarily a function of specific speed and specific diameter; this is shown in Figure 3 which is adapted from Figure 15 of reference 19. The remaining parameters must at least be accounted for.

While dimensional analysis suggested a Mach number influence in general, experience indicates that the crucial condition is in the relative flow at the rotor inlet. If the relative velocity exceeds the sonic speed, then shock wave patterns are created in the blade passages resulting in rapidly increasing losses. Figure 3 is limited, therefore to $M_{*w3} < 1$. Since this allows some slightly supersonic conditions in the absolute flow, say at the stator exit, it is not a stringent requirement for industrial machinery. The influence of the ratio of specific heats is not readily evident in references 19 and 20. Where it is mentioned at all in reference 19, $\gamma = 1.4$, the value for gases comprised of diatomic molecules. The small variation of γ with temperature will affect the efficiency to the extent of 2 to 4% perhaps but that is within the precision of the correlation, Figure 3. The large variation in γ comes with the atomic structure of the gas. Vavra,[21] for example, points out the great performance differences encountered when handling helium in nuclear power systems. For such a monatomic gas, $\gamma = 1.66$. However, the effects of large γ and the small molecular weight have not been sufficiently isolated to assign the contribution of each in modifying the diagram values of Figure 3.

Specific Speed:	$N_S = N(Q_4)^{1/2}/(H_{is})^{3/4}$
Specific Diameter:	$D_S = d_2(H_{is})^{1/4}/(Q_4)^{1/2}$
Isentropic Efficiency:	$\eta_T = (h_{03} - h_{04})/(h_{01} - h_{04'})$
Machine Reynolds Number:	$Re^* = u_3 d_3 \rho_4/\mu_4$
Rotor Inlet Relative Mach Number:	$M_{*w3} = w_3/a_{*3}$
Ratio of Specific Heats:	$\gamma = c_p/c_v$

Table 3. Dimensionless Parameters for Balje Stage Performance Correlation.

Of more common influence is the effect of the machine Reynolds number, Re^*. Comparing Figures 15 and 16 of reference 19 shows that the radial and axial turbine correlations are quite similar for $N_s > 10$ and adequately represented by our Figure 3 for $Re^* = 10^6$. The influence of Re^* on design point stage efficiency is described in Figure 4 where at $Re^* = 10^6$, the reference value of the isentropic efficiency is the diagram value from Figure 3. If, after using the stage specific speed and specific diameter to determine the efficiency, the machine Reynolds number $Re^* \neq 10^6$, the diagram efficiency should be modified as a function of N_s and Re^* from Figure 4. An elaboration of the Reynolds number effect appears in reference 22, and additional specific information is shown in Figure 3 of reference 27 (part B).

A word qualifying the use of the $N_s D_s$ correlation is desirable. While similarity analysis for correlating compressible fluid dynamic phenomena dates from the 1930's, Cordier[23] was perhaps the first to show that best performance of many turbomachines plotted on $N_s - D_s$ coordinates produced a locus of points approximating the ridge line on the efficiency contour map of Figure 3. Shepherd[9] gave the method and model which Balje[19] and

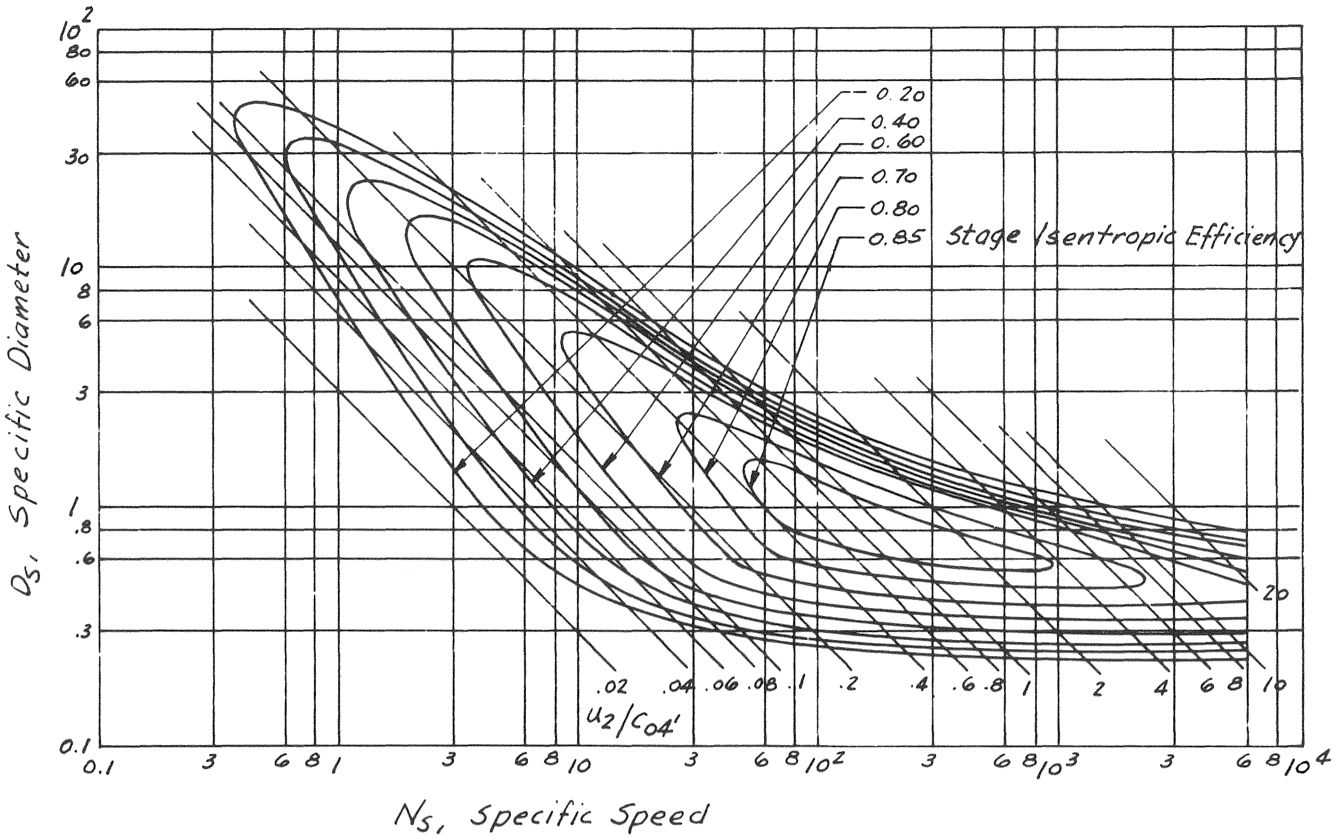

Figure 3. N_sD_s Diagram for Turbine Stage. Efficiency is on a total-to-total basis; that is, it is related to inlet and exit stagnation conditions. Diagram values are suitable for machine Reynolds number $Re^* \geq 10^6$.

Balje and Binsley[20] used in developing the details for the turbomachinery application. Borel[24] has carefully evaluated the basis on which such dimensional analysis is made and reference 25 gives an idea of the extent to which such work can be carried. Vavra[21] criticizes the approach by citing performance of actual turbomachine units which greatly exceeds the diagram values. This does not discredit either the method or Figure 3 but only emphasizes that each user must assemble his own data from experience and maintain the diagram up-to-date. In section G, the example of radial turbine stage synthesis was carried out partially based on the N_sD_s correlation of stage efficiency.

LOSS MECHANISMS

Information on the flow processes in the individual elements of a turbine stage is sufficiently complete that loss mechanisms may be described and actual flow conditions correlated with respect to apparently basic parameters. In this section the mechanisms will be identified and references where the correlations were formulated will be tabulated. In the next section, a procedure as consistent as can be devised at this time, will be presented for ascertaining the actual flow conditions based on the ideal conditions for both an axial turbine stage and a radial turbine. When time and knowledge allow, the element-by-element analysis of section F is to be preferred to the over-all correlation of stage performance given in section D.

Axial Turbine Loss Mechanisms

Losses in an axial turbine stage passage are associated with the blade profile, the passage sidewall or endwall, secondary flow, blade tip running clearance, flow incidence to the blade leading edge, and disk friction. The blade profile loss is due to boundary layer growth in the direction of flow. The loss is one of stagnation pressure due to a loss of momentum of the viscous fluid. The boundary layer growth, hence loss, very much depends on the profile shape and the pressure gradient to which the flow is subjected. The loss coefficient results from averaging the loss suffered in the boundary layer over all the flow in the passage. The endwall loss is again due to a loss of momentum in the boundary layer but it is clear that neither the pressure gradient nor the flow direction to which the endwall flow is subjected is the same as the profile flow. Despite this, the same loss coefficient is often used for both. More suitably, the endwall loss is combined with the secondary flow loss. Adjacent blade profiles produce both the desired exit flow conditions and a pressure gradient across the passage from pressure surface to suction surface. On opposite sides of the same blade the different pressure distributions produce the blade loading. Across the flow

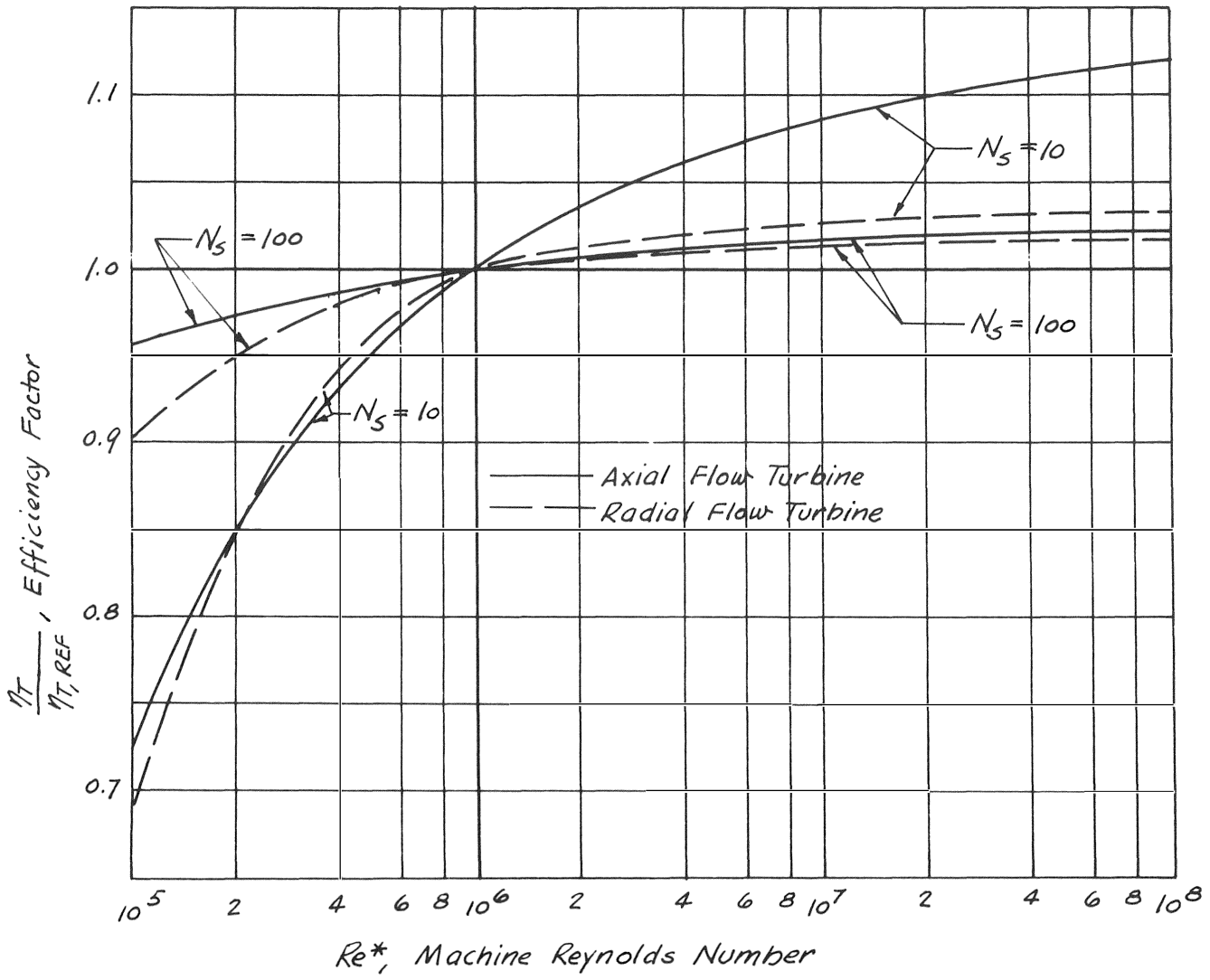

Figure 4. Influence of Reynolds Number on Turbine Stage Efficiency.

passage, the pressure gradient induces a component of flow from the higher to the lower pressure regions which is often identified as the secondary flow. It is synonymous with a three-dimensional boundary layer, is subject to complicated separation phenomena and results in the appearance of vorticity in the exit flow. Mechanically, the end of the moving (rotor) blades is free of the shroud casing. Pressure differences across the blade thickness then induce leakage flows through the clearance space. Pressure loss, turbulence and interference with the primary passage flow contribute to the tip clearance loss. Shock-free flow at the leading edge of the blade occurs when the gas angle and the blade angle coincide. When the gas angle varies from this condition, a component of the velocity perpendicular to the camber line is partially or wholly dissipated as a loss in kinetic energy. Finally, in the close clearance between rotor disk and casing diaphragm, the entrapped fluid is dragged about by the rotor and viscous dissipation becomes a power loss.

The mechanisms described above have been recognized and converted into correlations of the several losses whereby either the enthalpy or the stagnation pressure at the actual exit conditions is related to the same property which would be obtained at the conclusion of an isentropic process. For the axial turbine stage, the references where the correlations may be found are given in Table 4.

Radial Turbine Loss Mechanisms

The passages in a radial turbine stage suffer losses of the same nature as the axial stage. As mentioned previously, the radial turbine does not enjoy the same maturity as yet as the axial, hence not boundary layer considerations but rather pipe or channel friction loss effects are the basis for the nozzle passage and the rotor passage loss correlations. The rotor blade incidence and the disk friction give rise to losses identical to the axial

configuration. The rotor discharge loss is worth a separate note. In a single stage machine, the rotor discharge loss, associated with the unrecoverable kinetic energy of the exit flow, is often isolated from the stage performance and the isentropic efficiency is given on a total-to-static basis. Where the discharge kinetic energy is recoverable as in a multistage machine, the total-to-total basis for the efficiency is used.

The correlations of the radial turbine loss mechanisms appear in the literature as given in Table 4. Of all investigators, only Mizumachi[2] approaches the nozzle and rotor passage losses with an account of profile, endwall, and secondary effects. He then combines the results into an equivalent passage loss coefficient.

LOSS CORRELATIONS

Numerous attempts have been made to assemble correlations of the many loss effects into an over-all stage performance prediction method. We will present the Soderberg[32] correlation for the axial configuration because of its simplicity and unusual ability to predict actual results. The correlation has been applied by Stenning[33] and evaluated by Horlock,[1] Amann and Sheridan,[34] Lenherr and Carter,[35] and Brown[36] all of whom give it a slight preference over that of Ainley and Mathieson.[37] It must be said, however, that the latter correlation is much more elaborate and directed at two-dimensional design rather than the purposes of this paper.

The Soderberg axial turbine loss correlation is summarized in Table 5. The correlation is strictly applicable

Correlation includes effect of:	does not include:
Space - chord ratio, s/b	Mach number
Reynolds number, Re_h	Trailing edge thickness
Aspect ratio, H/b	Stagger angle
Thickness ratio, t_{max}/ℓ	
Blading geometry, ϵ or ϑ	

i) Determine optimum space-chord ratio to which correlation applies:

$$2(s/b)(\tan\alpha_2 + \tan\alpha_1)\cos^2\alpha_2 = 0.8 \text{ for optimum } s/b \qquad (37)$$

ii) Determine $\xi' = f(\epsilon, t_{max}/\ell)$ from Fig. 5a

iii) Calculate $\xi = \left(\frac{10^5}{Re_h}\right)^{1/4}\left[(1+\xi')(0.975 + 0.075\,\frac{b}{H}) - 1\right]$ (38)

where $Re_h = \rho_2 c_2 D_h/\mu_2$

$D_h = (2Hs\cos\alpha_2)/(s\cos\alpha_2 + H)$

iv) Modify ξ for rotor incidence loss (Fig. 5b)

v) Calculate actual endpoint enthalpy

$$h_2 = h_{2'} + \xi(c_2^2/2) \qquad (39)$$

Table 5. Soderberg Axial Turbine Loss Correlation.

			Loss Mechanisms for Axial Turbines					
Author	Date	Ref	Profile Loss	Endwall Loss	Secondary Flow Loss	Rotor Incidence	Tip Clearance	Wheel Disk Friction
Daily, Nece	1960	28						x
Mann, Marston	1961	29						x
Horlock	1966	1	x	x	x	x	x	
Balje, Binsley	1966	20	x	x			x	x
Balje	1968	26	x	Combined x			x	
Balje, Binsley	1968	27	x	Combined x			x	x

			Loss Mechanisms for Radial Turbines				
Author	Date	Ref	Nozzle Passage	Rotor Incidence	Rotor Passage	Rotor Discharge	Wheel Disk Friction
Balje	1952	7	x	x	x	x	x
Jamieson	1955	8	x		x	x	x
Mizumachi	1958	2	x	x	x	x	
Daily, Nece	1960	28					x
Knoerschild	1961	11	x	x	x		
Hiett, Johnston	1964	12	x		x		
Futral, Wasserbauer	1965	13	x	x	x		
Balje, Binsley	1968	2c	x	x	x		x
Rodgers	1966	31					x
Benson	1970	30	x	x	x		x

Table 4. Identification of Loss Mechanisms.

to conditions of an optimum space-chord ratio given by eq. (37). The departure of actual blading geometry from this condition should be checked. A loss coefficient ξ' is determined from Figure 5a as a function of the gas deflection and the blade maximum thickness. The effects of Reynolds number and aspect ratio are next introduced in eq. (38). Finally ξ is modified for an incidence loss using Figure 5b. The resulting loss coefficient then makes it possible to estimate the actual process endpoint enthalpy from the isentropic value as shown in eq. (39)

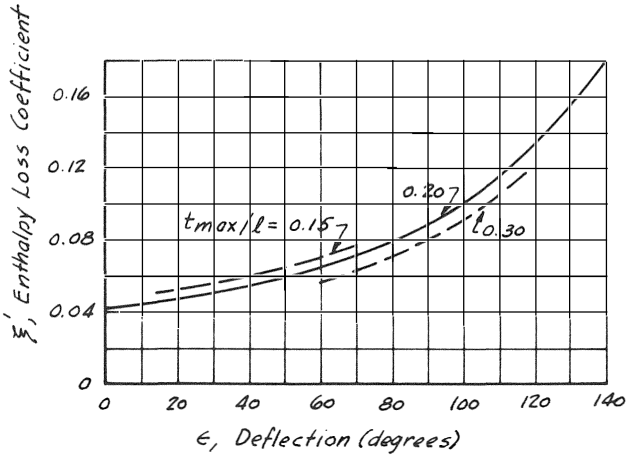

Figure 5a. Enthalpy Loss Coefficient for Use With the Soderberg Correlation.

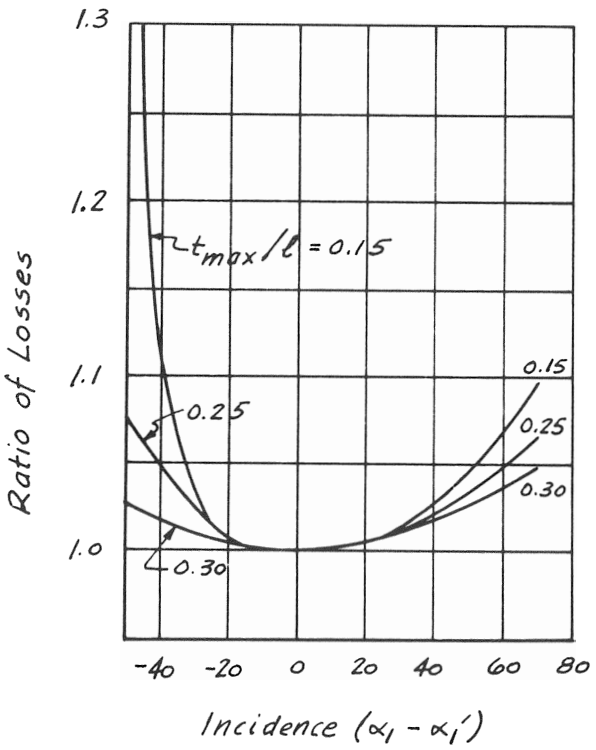

Figure 5b. Influence of Incidence on the Soderberg Loss Correlation.

and illustrated on Figure 2d. A subsequent correction of stage efficiency due to blade tip clearance is presented ambiguously in the literature and is not shown here. It must be realized that the Soderberg procedure applies to one passage. Where both stator and rotor passages occur in a stage, the procedure must be applied twice. Dixon[15] suggests that two forms of eq. (38) be used, one for rotors, one for stators but this is confirmed by no other author. Finally eq. (39) involves the actual exit velocity which usually cannot be determined until the enthalpy is known. Clearly then solution of eq. (39) requires iteration over the process calculations but in the writer's experience convergence is achieved in the second, at most third loop.

Correlation of the loss effects in a radial turbine stage is much less complete and has been subject to far less critical evaluation than that of the axial turbine. Reports of three important experimental programs dealing with radial turbines exist; the D.I.G.T. work in England,[12,30] the Japanese industrial program,[2,18] and the NASA space power package program in the USA of which the work of reference 13 is part. Of these three programs, Benson[30] presents a consistent loss correlation at the level of the presentation of this paper. The procedure is summarized in Table 6.

A nozzle loss coefficient is first determined from Figure 6a as a function of the discharge Mach number. The actual nozzle endpoint enthalpy can be determined iteratively by eq. (40). Figure 6b then yields the rotor incidence loss coefficient which combined with the actual gas angles in eq. (41) leads to the actual rotor inlet

Correlation includes effect of:

Nozzle passage

Rotor blade incidence

Rotor passage including fluid friction, clearance, disk friction

i) Determine nozzle loss coefficient ξ_N from Fig. 6a or use $\xi_N = 0.1$

ii) Calculate actual nozzle endpoint enthalpy

$$h_2 = h_{2'} + \xi_N (c_2^2/2) \tag{40}$$

iii) Determine rotor incidence loss coefficient Y_{SH} from Fig. 6b

iv) Calculate the enthalpy ratio s:

$$s = \frac{(\tan^2\beta_2 + 1) - Y_{SH}}{\sec^2\beta_3} \tag{41}$$

and the actual rotor inlet enthalpy

$$h_3 = s h_2 \tag{42}$$

v) Calculate the rotor passage loss coefficient ξ_{RB}:

$$\xi_{RB} = mk\left[1 + (w_3/w_4)^2\right] \tag{43}$$

where $mk = 0.468$ (Benson, 1970)
$mk = 0.442$ (Futral, et al. 1965)

and $$h_4 = h_{4'} + \xi_{RB}(w_4^2/2) \tag{44}$$

Table 6. Benson Radial Turbine Loss Correlation.

enthalpy, eq. (42). The basis for the rotor passage loss coefficient is the work of Futral and Wasserbauer;[13] the analysis of the experimental data in references 13 and 30 leads to very similar values of the parameter in eq. (43). The final endpoint enthalpy at the rotor exit is again

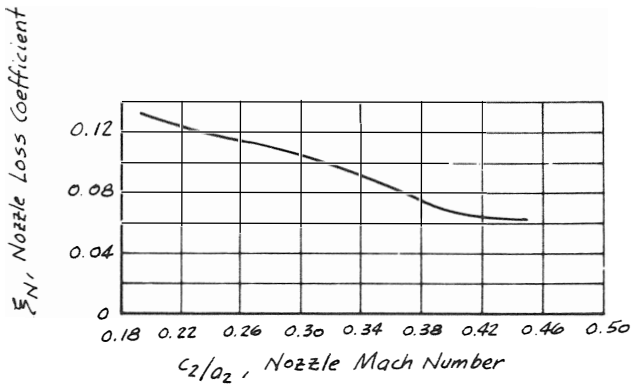

Figure 6a. Nozzle Enthalpy Loss Coefficient for the Benson Correlation.

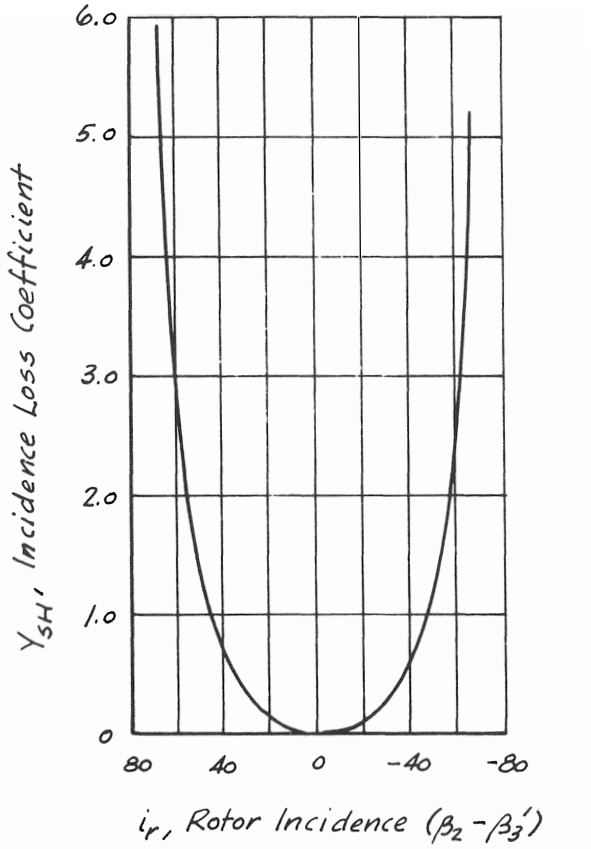

Figure 6b. Rotor Inlet Shock Loss for the Benson Correlation.

determined iteratively by eq. (44). Note that relative velocities, w, are used in the rotor correlation.

STAGE ANALYSIS OR SYNTHESIS

In drawing this presentation of turbine aerodynamic performance including losses to a close, it will be helpful to show a tabulation in which the results of synthesis of a radial turbine stage are given in detail. Only results are shown in Table 7 and these may prove a guide to the conscientious worker in applying his knowledge of compressible fluid dynamics together with the loss correlations shown in this paper. At the left top of the table is included the information necessary to begin the calculation. At the top right are over-all stage parameters which come out of the procedure while the flow conditions calculated for the four stations in the turbine stage comprise the remainder of the table.

Results such as shown in Table 7 and as are yielded by all of the correlations introduced in this paper are to be designated on-design-point conditions for the turbine stages considered. Some of the fluid mechanic calculations for on-design-point estimates are illustrated in references 13, 38 and 39. It was pointed out by Benson[30] that his correlation as well as that of reference 13 was very useful in off-design-point estimates of stage performance as well but such predictions are outside the scope of this paper.

REFERENCES

1. Horlock, J. H., *Axial Flow Turbines*, Butterworth and Co., Ltd., London (1966).
2. Mizumachi, N., "A Study of Radial Turbines," Institute of Industrial Science, University of Tokyo (Dec. 1958) (English translation: Industry Program Report No. IP-476, University of Michigan, Ann Arbor (Nov. 1960); copy obtainable from university library).
3. Shapiro, A. H., *The Dynamics and Thermodynamics of Compressible Fluid Flow*, Vol. I, The Ronald Press Co. (1953).
4. Daily, J. W., Harleman, D. R. F., *Fluid Dynamics*, Addison-Wesley Publishing Co., Inc., (1966).
5. Owczarek, J. A., *Introduction to Fluid Mechanics*, International Textbook Co., (1968).
6. Thompson, P. A., *Compressible-Fluid Dynamics*, McGraw-Hill Book Co., (1971).
7. Balje, O. E., "Contribution to the Problem of Designing Radial Turbomachines," *ASME Transactions, 74.* pp. 451-472 (1952).
8. Jamieson, A. W. H., "The Radial Turbine," Chapter 9, *Gas Turbine Principles and Practice*, D. VanNostrand Co., Inc. (1955).
9. Shepherd, D. G., *Principles of Turbomachinery*, The Macmillan Co. (1956).
10. Wallace, F. J., "Theoretical Assessment of the Performance Characteristics of Inward Radial Flow Turbines," *Proceedings, Inst. of Mechanical Engineers, 172*, pp 931-952 (1958).
11. Knoernschild, E. M., "The Radial Turbine for Low Specific Speeds and Low Velocity Factors," *Journal Engineering for Power, ASME Transactions, 83A*, pp 1-8 (1961).
12. Hiett, G. F., and Johnston, I. H., "Experiments Concerning the Aerodynamic Performance of Inward-Flow Radial Turbines," *Proceedings, Inst. of Mechanical Engineers, 178*, part 3I, pp 28-42 (1963).
13. Futral, S. M., Wasserbauer, C. A., "Off-design Performance Prediction with Experimental Verification for a Radial-inflow Turbine," Report TND-2621, NASA (Feb. 1965).
14. Wilson, D. G., Jansen, W., "The Aerodynamic and Thermodynamic Design of Cryogenic Radial-inflow Expanders," Paper 65-WA/PID-6, ASME (Nov. 1965).
15. Dixon, S. L., "Radial Flow Turbines," Chapter 8, *Fluid Mechanics, Thermodynamics of Turbomachinery*, Pergamon Press (1966).
16. Jansen, W., Qvale, E. B., "A Rapid Method for Predicting the Off-design Performance of Radial-inflow Turbines," Paper 67-WA/GT-3, ASME (Nov. 1967).
17. Vavra, M. H., "Radial Turbines," Pt. 4, *AGARD-VKI Lecture Series on Flow in Turbines* (Series #6), Von Karman Institute for Fluid Dynamics (March 1968).

INPUT DATA (TYPE 2)		STAGE PARAMETERS	
MASS FLOW RATE (LBM/SEC)	0.469	SP HT(PRESS)(FT2/SEC2-OR)	6903.3
INLET STAG TEMP (OR)	2010.0	RATIO OF SPECIFIC HEATS	1.331
INLET STAG PRESS (PSIA)	30.90	TURBINE MACH NO	0.719
GAS CONS (FT2/SEC2-OR)	1716.47	TURBINE REYNOLDS NO	933986.
STAGE STAG PRESS RATIO	1.937	ISENTROPIC WORK (BTU/LBM)	84.01
NOZZLE INLET MACH NO	0.100	ACTUAL WORK OUT (BTU/LBM)	69.52
ROTOR IN ABS FLOW ANGLE (DEG)	19.98	ISEN STAGE EFF (TOT TO TOT)	0.8275
MINIMUM SLIP FACTOR	0.850	NOZZLE EFFICIENCY	0.8509
ROTOR OUT ABS FLOW ANGLE (DEG)	90.00	ROTOR EFFICIENCY	0.8839
ROTOR OUT BLADE EDGE ANGLE (DEG)	90.00	DEGREE OF REACTION	0.5179
ROTOR OUT REL CRIT MACH NO	0.535	NO NOZZLE BLADES	12
ROTOR OUT HUB DIAMETER (IN)	2.000	NOZZLE BLADE LENGTH (IN)	3.211
SPECIFIC SPEED	63.302	SLIP FACTOR	0.856
SPECIFIC DIAMETER	1.684	NO ROTOR BLADES	16
ROTOR SPEED (RPM)	58000.0	ROTOR TIP BLADE ANGLE (DEG)	90.80
ROTOR TIP DIAMETER (IN)	5.640	ROTOR DIAMETER RATIO	1.737

FLOW CONDITIONS STATION	NOZZLE IN (1)	NOZZLE OUT (2)	ROTOR IN (3)	ROTOR OUT (4)
STAG PRESSURE (PSIA)	30.90	29.74	29.52	15.95
STAG TEMPERATURE (OR)	2010.0	2010.0	2010.0	1757.9
STAG ENTHALPY (BTU/LBM)	554.22	554.22	554.22	484.70
MACH NUMBER (STAG)	0.100	0.582	0.605	0.279
STAG SOUND VELOCITY (FT/SEC)	2142.9	2142.9	2142.9	2004.0
STAG DENSITY (LBM/FT3)	0.0415	0.0399	0.0396	0.0245
PRESSURE (PSIA)	30.70	23.58	22.97	15.14
TEMPERATURE (OR)	2006.7	1897.3	1888.4	1735.3
ENTHALPY (BTU/LBM)	553.31	523.16	520.71	478.48
MACH NUMBER (STATIC)	0.100	0.599	0.624	0.280
SOUND VELOCITY (FT/SEC)	2141.1	2082.0	2077.1	1991.1
DENSITY (LBM/FT3)	0.0413	0.0336	0.0328	0.0236
DYNAMIC VISCOSITY (LBM/FT-SEC)	2.97E-05	2.86E-05	2.85E-05	2.70E-05
CRITICAL SOUND VELOCITY (FT/SEC)	1984.9	1984.9	1984.9	1856.3
MASS FLOW RATE (LBM/SEC)	0.469	0.469	0.469	0.469
VOLUME FLOW RATE (FT3/SEC)	11.359	13.979	14.284	19.910
NOZZLE INLET DIAMETER (IN)	10.074			
NOZZLE EXIT DIAMETER (IN)		5.922		
IMPELLER INLET DIAMETER (IN)			5.640	
BLADE EXIT, HUB DIAMETER (IN)				3.246
BLADE EXIT, SHROUD DIAMETER (IN)				3.246
PASSAGE WIDTH (IN)	0.299	0.299	0.286	0.504
CROSS-SECTION AREA (IN2)	9.182	4.879	4.640	5.135
ABSOLUTE VELOCITY, C (FT/SEC)	214.1	1247.1	1295.4	558.3
PERIPHERAL VELOCITY, U (FT/SEC)			1427.3	821.5
RELATIVE VELOCITY, W (FT/SEC)			489.7	
SHROUD RELATIVE VELOCITY, WS (FT/SEC)				993.3
RELATIVE CRITICAL MACH NUMBER			0.247	0.535
ABSOLUTE FLOW ANGLE (DEG)	56.30	19.32	19.98	90.00
RELATIVE FLOW ANGLE, SHROUD (DEG)			64.87	34.20
RELATIVE FLOW ANGLE, HUB (DEG)			64.87	34.20
ENTROPY GAIN (STAG)		65.590	12.731	131.335

Table 7. Example: Radial Turbine Stage Synthesis.

18. Watanabe, I., Ariga, I., Mashimo, T., "Effect of Dimensional Parameters of Impellers on Performance Characteristics of a Radial-inflow Turbine," *Journal Engineering for Power, ASME Transactions, 93A*, pp 81-102 (1971).

19. Balje, O. E., "A Study on Design Criteria and Matching of Turbomachines: Part A — Similarity Relations and Design Criteria of Turbines," *Journal, Engineering for Power, ASME Transactions, 84A*, pp 83-102 (1962).

20. Balje, O. E., Binsley, R. L., "Turbine Performance Prediction: Optimization Using Fluid Dynamic Criteria," Report R-6805, Rocketdyne Div., North American Aviation, Inc. (Dec. 1966) (NTIS AD-642767).

21. Vavra, M. H., "Basic Elements for Advanced Designs of Radial-flow Compressors," *Advanced Compressors*, Lecture Series #39, AGARD-NATO (Aug. 1970).

22. *Reynolds Number Symposium, Journal, Engineering for Power, ASME Transactions, 86A*, pp 225-298 (1964).

23. Cordier, O., "Ähnlichkeitsbedingungen für Strömungsmachinen," *Brennstoff, Warme Kraft, 5*, pp 337-340 (1953); see also *VDI Bericht, 3*, pp 85-88 (1955).

24. Borel, L., "Characteristic Dimensionless Figures for Turbomachines," *Water Power, 19*, pp 494-498 (1967); *20*, pp 27-32 (1968).

25. Wislicenus, G. F., "Turbomachinery Design Described by Similarity Considerations," Symposium, Fluid Mechanics and Design of Turbomachinery, Pennsylvania State University (Aug. 1970); to be published in NASA SP.

26. Balje, O. E., "Axial Cascade Technology and Application to Flow Path Design," *Journal, Engineering for Power, ASME Transactions, 90A*, pp 309-340 (1968).

27. Balje, O. E., Binsley, R. L., "Axial Turbine Performance Evaluation," *Journal, Engineering for Power, ASME Transactions, 90A*, pp 341-360 (1968).

28. Daily, J. W., Nece, R. E., "Chamber Dimension Effects on Induced Flow and Frictional Resistance of Enclosed Rotating Disks," *Journal of Basic Engineering, ASME Transactions, 82D*, pp 217-232 (1960).

29. Mann, R. W., Marston, C. A., "Friction Drag on Bladed Disks in Housings as a Function of Reynolds Number, Axial and Radial Clearance and Blade Aspect Ratio and Solidity," *Journal of Basic Engineering, ASME Transactions, 83D*, pp 719-723 (1961).

30. Benson, R. S., "A Review of Methods for Assessing Loss Coefficients in Radial Gas Turbines," *International Journal of Mechanical Sciences, 12*, pp 905-932 (1970).

31. Rodgers, C., "Efficiency and Performance Characteristics of Radial Turbines," Paper 660754, SAE Oct. (1966).

32. Soderberg, C. R., Unpublished Report, Gas Turbine Laboratory, MIT (1949).

33. Stenning, A. H., "Design of Turbines for High Energy Fuel, Low Power Output Applications," Report 79, Dynamic Analysis and Control Laboratory, MIT (1953).

34. Amann, C., and Sheridan, D. C., "Comparisons of Some Analytical and Experimental Correlations of Axial-flow Turbine Efficiency," Paper 67-WA/GT-6, ASME (Nov. 1967).

35. Lenherr, F. K., Carter, A. F., "Correlation of Turbine Blade Total-Pressure-Loss Coefficients Derived from Achievable Stage Efficiency Data," Paper 68-WA/GT-5, ASME (1968).

36. Brown, L. E., "Axial Flow Compressor and Turbine Loss Coefficients: A Comparison of Several Parameters," *Journal, Engineering for Power, ASME Transactions, 94A*, pp 193-201 (1972).

37. Ainley, D. G., Mathieson, G. C. R., "A Method of Performance Estimation for Axial Flow Turbines," R and M 2974, Aeronautical Research Council (1957).

38. Benson, R. S., "Predictions of Performance of Radial Gas Turbines in Automotive Turbochargers," Paper 71-GT-66, ASME (March 1971).

39. Scheel, L. F., Cline, R. F., Perkins, E. S., "Technology for Centrifugal Compressors," Paper 71-PET-24, ASME (Sept. 1971).

NOMENCLATURE

A	cross-sectional area
a	area
a	sonic velocity based on local conditions
a_*	sonic velocity based on critical conditions, i.e., conditions where local velocity just equals sonic velocity, thus where $c = a = a_*$
b	blade length (see Figure 2c)
c	absolute velocity
$\overline{c}$	vector of the absolute fluid velocity (see Figure 1)
c_m	component of absolute fluid velocity in meridional plane
c_u	component of absolute fluid velocity perpendicular to meridional plane
c_p	specific heat at constant pressure of flowing fluid
c_v	specific heat at constant volume of flowing fluid
D_h	hydraulic diameter (see Table 5)
D_s	specific diameter (see Table 3)
d	diameter
d_s	shroud diameter (see Figure 2a)
d_h	hub diameter (see Figure 2a)
E	energy of system (see Table 1c)

e	internal energy (thermodynamic property)
$\bar{F}$	vector force
$\bar{g}$	gravitational acceleration
$\bar{H}$	angular momentum of system (see Table 1d)
H_{is}	isentropic work extraction $(= h_{o1} - h_{o'_1})$
H	blade height
h	enthalpy (thermodynamic property)
$\bar{i}, \bar{j}, \bar{k}$	unit vectors in the coordinate directions (see Figure 1)
i	incidence (see Figure 2c)
l	blade chord (see Figure 2c)
$\bar{M}$	moment
M	mass of system (see Table 1a)
M_{*w}	relative Mach number based on critical conditions
$\mathring{m}$	mass flow rate (see Table 1a)
N_s	specific speed (see Table 3)
N	rotative speed
n	polytropic exponent
$\bar{n}$	outward drawn unit normal vector (see Figure 1)
$\bar{p}$	linear momentum of system (see Table 1b)
p	pressure (thermodynamic property)
Q	volume flow rate or capacity
Q	heat transfer with respect to the system
R	radius from axis of rotation (see Figure 1)
Re^*	machine Reynolds number (see Table 3)
Re_h	Reynolds number based on passage hydraulic diameter (see Table 5)
R_H	reheat factor (see Table 2b)
$\bar{r}$	radius vector (see Figure 1)
r	degree of reaction of turbine stage (see Table 2a)
r, ϑ, z	orthogonal, cylindrical coordinate system (see Figure 1)
S	surface area of control volume
s	coordinate along streamline
s	entropy (thermodynamic property)
s	blade pitch or spacing (Figure 2c)
$\bar{T}$	torque
T	temperature (thermodynamic property)
t	time
t_{max}	blade thickness (see Figure 2c)
u	blade or rotor tip velocity
u, v, w	components of c in the three coordinate directions (see Figure 1)
V	volume of control volume
v	volume
W	work transfer with respect to the system
w	relative fluid velocity
w_m	component of the relative fluid velocity in meridional plane
w_u	component of the relative fluid velocity perpendicular to meridional plane
Y_{sH}	shock loss coefficient (see Figure 6b)
α	stator gas angle (see Figure 2c)
α'	stator blade angle (see Figure 2c)
β	rotor gas angle (see Figure 2c)
β'	rotor blade angle (see Figure 2c)
γ	stagger angle (see Figure 2c)
γ	ratio of specific heats
δ	blade edge angle (see Figure 2a)
δ	deviation (see Figure 2c)
ϵ	energy/unit mass (see Table 1c)
ϵ	deflection (see Figure 2c)
η_N	nozzle (stator) efficiency (see Table 2a)
η_R	rotor efficiency (see Table 2a)
η_T	turbine stage isentropic efficiency (see Table 2a)
η_s	small stage efficiency (see Table 2b)
η_{PT}	turbine stage polytropic efficiency (see Table 2b)
ϑ	camber (see Figure 2c)
μ	dynamic viscosity
ξ	loss coefficient based on enthalpy (see Table 5)
ξ_N	nozzle loss coefficient (see Figure 6a)
ξ_{RN}	rotor loss coefficient (see Table 6)
ρ	density (thermodynamic property)
Ψ	gravitational potential
Ω	rotor angular velocity (see Figure 1)
∇	vector operator $(= \partial/\partial r\,\bar{i} + 1/r\ \partial/\partial\vartheta\,\bar{j} + \partial/\partial z\,\bar{k})$
ln	logarithm to base e

Subscripts

1, 2, 3, 4	turbine stage station numbers (see Figure 2)
o	local stagnation conditions which are obtained when
s	stator
r	rotor